Streamlining Information Transfer between Construction and Structural Engineering
Edited by Shiau, J., Vimonsatit, V., Yazdani, S., and Singh, A.

ISBN: 978-0-9960437-7-9

HYSTERESIS CHARATERISTICS OF SQUARE CFT COLUMNS SUBJECTED TO AXIAL FORCE AND BENDING MOMENT

KOUTA JYOUZAKI and MASAE KIDO

Dept of Architecture, the University of Kitakyushu, Kitakyushu, Japan

Hysteresis characteristics of concrete filled steel tubular columns have been proposed. However, it has not been clarified if the skeleton curve could be applied for slender columns, and there are few studies about the unloading stiffness of the hysteresis loop. The purpose of this study is to compare the skeleton curves of square CFT columns, which have been proposed by the moment-rotation angle relationships and the experimental data by the previous research. The relationship between the initial stiffness obtained by the theoretical calculation and the unloading stiffness obtained by the experimental study are shown. Also the effects of the axial force ratio and the width-thickness ratio on the above mentioned relationships are discussed. The loading condition of the experimental study is monotonic and cyclic loading. It is found that the skeleton curve evaluates conservatively the bending moment-rotation angle relationships obtained by the test in both loading conditions, except for the width-thickness ratio 43 specimen with cyclic loading. The ratio of unloading stiffness ${}_{ex}K_r$ obtained from the experimental data and calculated theoretical stiffness K was shown. The effect of the axial force ratio on the ${}_{ex}K_r/K$ was observed when the rotation chord angle was more than 1% and the width-thickness ratio increased as ${}_{ex}K_r/K$ decreased.

Keywords: Theoretical stiffness, Skeleton curve, Width-thickness ratio, Unloading stiffness, Monotonic loading, Cyclic loading.

1 INTRODUCTION

The factors which effects the hysteresis characteristics of concrete filled steel tube columns (hereinafter CFT) are the width-thickness ratio, axial force ratio, the effective length-depth ratio, strength of steel tube and concrete, etc. Furthermore, for the reasonable performance design, it is necessary to formulate the hysteresis characteristics that can consider the damage condition and the parameters mentioned above, which affect the structural performance.

There are several studies on the skeleton curve and hysteresis rule of CFT columns. Among them, the model of hysteresis characteristics with wide application range proposed by the U.S.-Japan research program (Mori *et al.* 1998) is shown in the Recommendations for design and Construction of Concrete Filled Steel Tubular Structures (hereafter CFT Recommendations) (AIJ 2008). The skeleton curve is a normal trilinear type model. According to the CFT Recommendations, the skeleton curve and the hysteresis rule correspond well to the experimental data, however, the strength evaluates conservatively the experimental strength and the hysteresis energy absorption is overestimated when the rotation angle is more than 1%. There are few studies about the unloading stiffness of CFT columns and clarifying the unloading stiffness is

important for evaluating appropriately the hysteresis energy absorption when the rotation angle of CFT columns is large.

In this study, the skeleton curves are compared with the experimental data of the square CFT columns subjected to the constant axial force and lateral force. Furthermore, the relation between the initial stiffness based on the theory and the unloading stiffness are shown and the effect of the width-thickness ratio and axial force ratio is shown.

2 INFLUENCE OF AXIAL FORCE RATIO, WIDTH-THICKNESS RATIO, CONCRETE STRENGTH ON SKELETON CURVE

2.1 Outline of the Proposed Skeleton Curve

This section outlines the skeleton curve of the CFT column shown in AIJ CFT Recommendations. Figure 1 shows a schematic diagram of a skeleton curve. The first break point is the yield strength M_Y, and the second break point is the ultimate strength M_U according to the CFT Recommendations. The theoretical initial stiffness is calculated by assuming that the total cross-section is elastic. The stiffness reduction rate α_Y is 0.7. In addition, the limit rotation angle R_U is defined as the rotation angle when the maximum strength is reduced by 95%, and it is expressed by the Eq. (1). Where, in the Eq. (1), γ_r is 1 when L_k/D is less than or equal to 10 and is 0.8 when L_k/D is larger than 10. In Eq. (1), β is defined by Eq. (2).

$$R_U(\%) = \frac{\gamma_r \times 100}{0.15 + 3.79\dfrac{N}{N_0}} \cdot \frac{t}{D} \cdot \beta \tag{1}$$

$$\beta = 1.0 - \frac{{}_c\sigma_B - 40.3}{566} \le 1.0 \tag{2}$$

Where, N is the axial force, N_0 is the compressive strength, D is the section width, t is the plate thickness and ${}_c\sigma_B$ is the concrete strength.

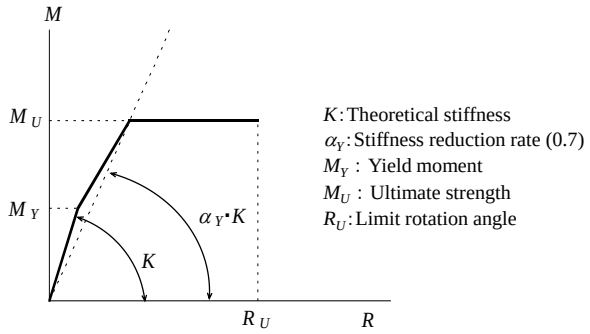

Figure 1. Skeleton curve of the CFT column defined in CFT Recommendation.

2.2 Effect of the Parameters

The skeleton curve shown in the previous section was calculated by selecting the following parameters for square cross sections.

- Axial force ratio n ($=N/N_0$): 0, 0.1, 0.2, 0.3, 0.4, 0.5, 0.8
- Width-thickness ratio D/t: maximum value of FA and FC rank

- Concrete strength ${}_c\sigma_B$ (N/mm^2): 24, 60

In addition, the depth D of the cross section is and 500 mm, the effective length-depth ratio L_k/D (L_k: effective length) is 12 and the steel tube F value is 325 N/mm^2. The width-thickness ratio's rank is defined in the Technical requirements for structural safety (MLIT 2015).

Figure 2 shows the skeleton curves when the concrete strength is 24 and 60N/mm^2 and the width-thickness ratio is the FA and FC rank. Some limit rotation angle R_U exceed 5% and it is expressed by arrows in the figure.

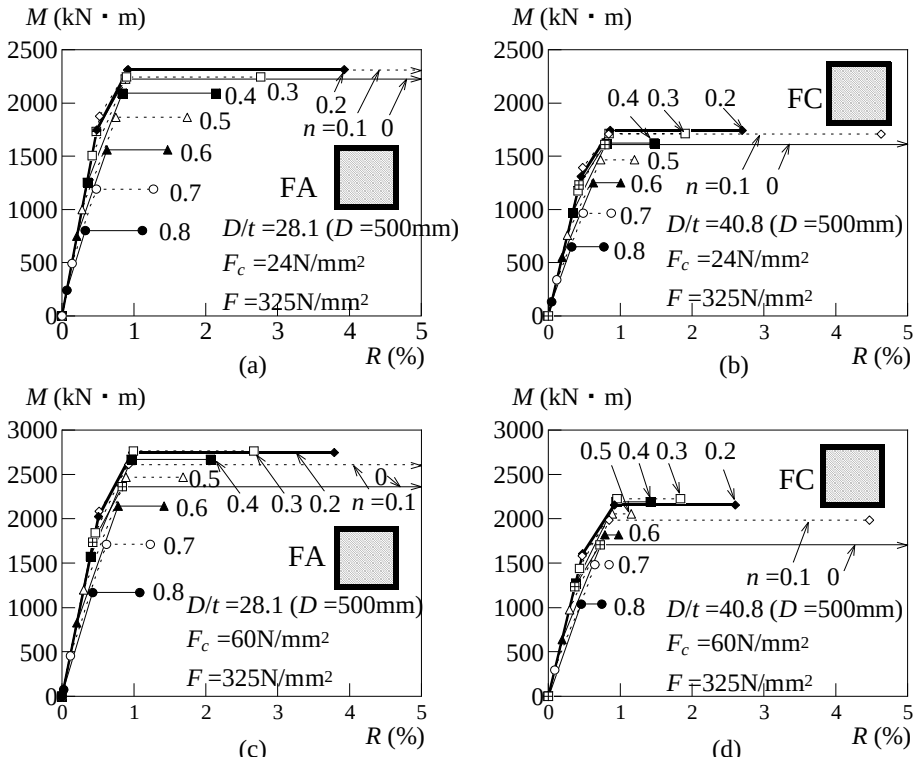

Figure 2. Influence of axial force ratio, width-thickness ratio and concrete strength on skeleton curve.

3 COMPARISON OF PAST EXPERIMENT RESULTS

3.1 Outline of the Experimental Study

Results of the previous experimental study are used. As shown in Figure 3, the loading condition is a cantilevered column which is one end fixed and other end free and subjected to the constant axial force N and lateral force Q.

In Table 1, No.1~No.3 series specimen's L_k/D is 10 (Matsui *et al.* 1998) and No.4 series specimen's L_k/D is 20 (Jyouzaki *et al.* 2018). The effective length L_k is equal to $2L$. The experimental parameters of No.1 ~ No.3 series are the width-thickness ratio D/t of the steel tube, the axial force ratio n, and the loading program. The cyclic loading program is shown in Figure 4 and the rotation angle of the column R ($=\delta/L$, δ: lateral displacement) is increased by 0.25% every four cycles. The experimental parameter of No.4 series is the axial force ratio n, and the loading program is monotonic loading.

The steel tube used in the experiment is a square steel tube of STKR 400 (Japanese Industrial Standard) and BCR295. The measured dimensions of the steel tube are shown in Table 1, the

results of the tensile test of the steel tube and the concrete compressive strength are shown in Table 2.

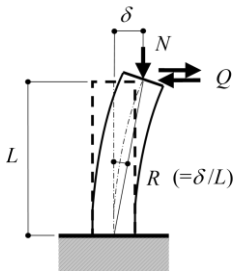

Figure 3. Loading condition.

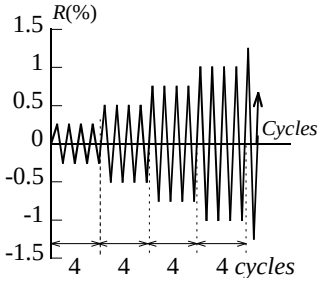

Figure 4. Loading program.

Table 1. Measured dimension of steel tube.

Series No.	Diameter ratio	L_k/D	Section depth D (cm)	Thickness t(mm)	D/t	Sectional area ${}_sA$ (cm^2)
1	22	10	10.0	4.40	22.7	16.3
2	31	10		3.21	31.1	12.2
3	43	10		2.24	44.6	8.6
4	25	20	15.0	5.97	25.1	33.3

Table 2. Tension test results and concrete strength.

Series No.	Diameter ratio	Steel tube	Yield stress ${}_s\sigma_y$ (N/mm^2)	Tensile strength σ_u (N/mm^2)	Concrete strength ${}_c\sigma_B$ (N/mm^2)	
					R*	M*
1	22	STKR	407	463	34.1	36.3
2	31	STKR	449	505	36.0	36.3
3	43	STKR	415	465	36.2	36
4	25	BCR	378	457	-	55.1~61.6

Note: *R: cyclic loading, M: monotonic loading

3.2 Comparison of Experiment Results

3.2.1 *In case of monotonic loading*

Figure 5 shows the bending moment M-rotation angle R relationship obtained by the experimental study and the calculated skeleton curves. The bending moment is calculated as $M = Q \cdot L + N \cdot \delta$ ($\delta = RL$). In the figure, the square marks indicate the point where the strain at the outer edge reaches the yield strain by the tensile test for the first time (steel tube yield), the arrows indicate the point where the local buckling occured and the circle marks indicate the maximum bending strength. When the L_k/D=20 and n=0.45 and 0.6, the limit rotation angle R_u calculated by Eq. (1) are smaller than the second break point's rotation angle.

According to the figure, the ultimate strength of the skeleton curve evaluates conservatively the experimental value except for the case of D/t=43 and n=0.5. In case of the D/t=43, n=0.3 and L_k/D=20, n=0.45 and n=0.6, the ultimate strength of the skeleton curve is almost same as the experimental maximum load. As for the lateral stiffness, in case of L_k/D=20, the skeleton curve's

stiffness is larger than that of the experiment. This is because that these specimens are slender and the first breaking point strength is larger than the actual one and the reduction of the stiffness after the concrete cracking are not considered.

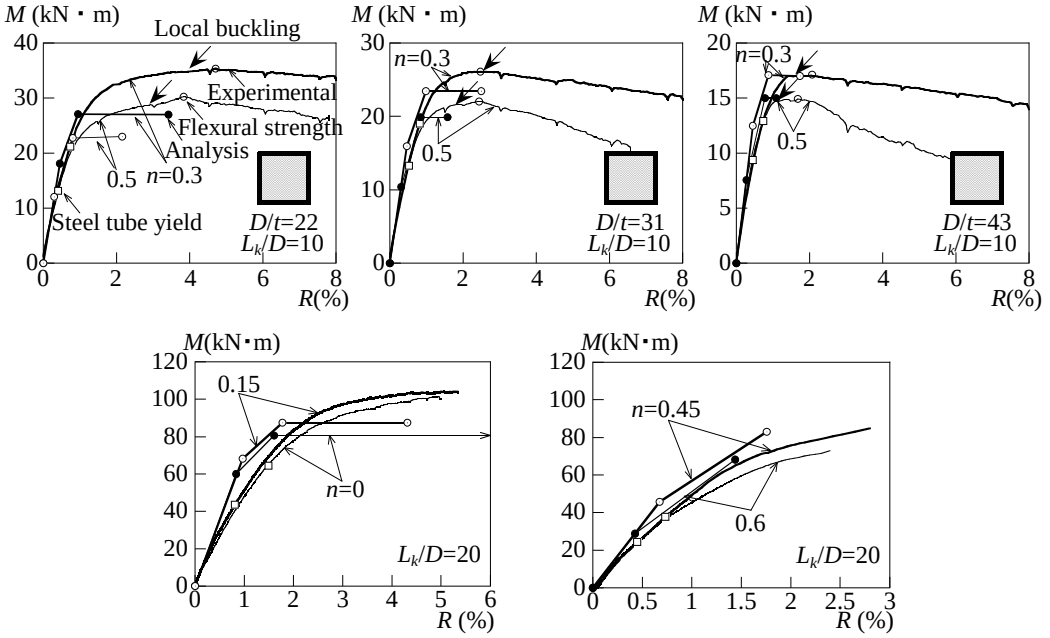

Figure 5. Comparison between experimental value and calculated value (Monotonic loading).

3.2.2 *In case of cyclic loading*

Figure 6 shows the comparison between the *M-R* relationship and the skeleton curve in the case of the axial force ratio n=0.3. The dotted line in the figure shows the result of monotonic loading. When the width-thickness ratio is 43, the experimental strength is smaller than the calculated ultimate strength.

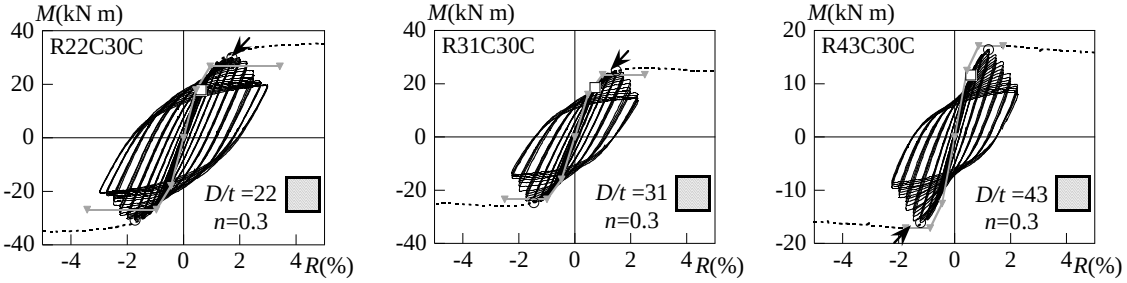

Figure 6. Comparison between experimental value and calculated value (Cyclic loading).

4 INITIAL STIFFNESS AND UNLOADING STIFFNESS

Unloading stiffness ${}_{ex}K_r$ was obtained from experimental data. Where, the values of the experienced rotation angle and the residual rotation angle obtained by Kido and Tsuda (2005) were used.

Figure 7 shows the ratio of the unloading stiffness and the theoretical stiffness K. The axial force ratio is 0.3 and 0.5. The ratio ${}_{ex}K_r/K$ decreases as the rotation angle increases. The effects of the axial force ratio is observed after the rotation angle exceeding 1%, and the value of ${}_{ex}K_r/K$ in case of n=0.5 is smaller than those of n=0.3. The value of ${}_{ex}K_r/K$ is smaller in case of D/t=43 than those of D/t=22 and 31.

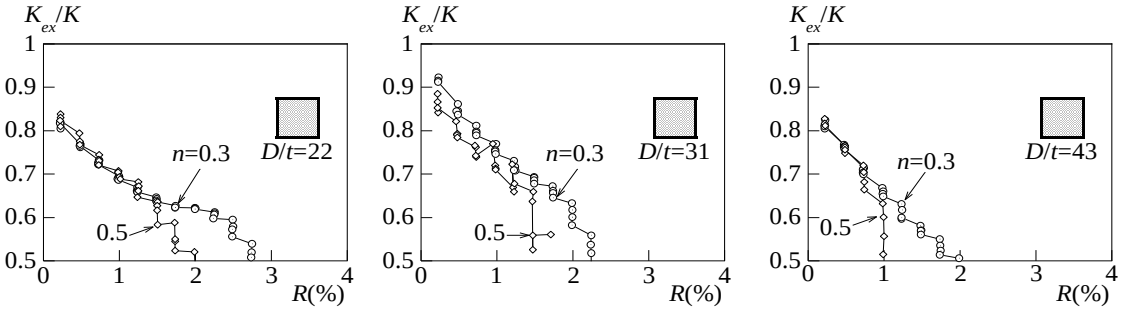

Figure 7. Comparison between experimental value and calculated value (Cyclic loading).

5 CONCLUSIONS

The conclusions derived from this study are as follows:

- The skeleton curves shown in AIJ CFT Recommendation were compared with the moment-rotation angle relationship obtained by the experimental study. The ultimate strength of the skeleton curves evaluate well except for the D/t=43 and n=0.5 specimen in monotonic loading and D/t=43 and n=0.3 specimen in cyclic loading. The lateral stiffness of the skeleton curves disagree with the test results in case of specimens with L_k/D=20.
- The relationship between the theoretical stiffness and the unloading stiffness obtained by the experimental study were shown. The effects of the axial force ratio is observed after the rotation angle exceeding 1%.

References

AIJ, *Recommendations for Design and Construction of Concrete Filled Steel Tubular Structures (in Japanese)*, Architectural Institute of Japan, Japan, 2008.

Jyouzaki, K., Kido, M., Fujioka, D., and Tsuda, K., *Study on The Fatigue Properties of Slender Square CFT Columns under Cyclic Lateral Loading with Constant Deflection Part 3 in The Case Of L_k/D=20 Specimens Subjected to High Axial Force (in Japanese)*, AIJ Kyushu Chapter Architectural Research Meeting, No. 57, Japan, March, 2018.

Kido, M. and Tsuda, K., Relation between Experimental Lateral Drift Angle and Residual One of Concrete Filled Steel Square Tubular Column (in Japanese*)*, *Steel Structure Annual*, Vol. 13, pp.503-508, November, 2005.

Matsui, C., Tsuda, K., Yamaji, Y., and Fujinaga, T., Structural Performance and Axial Force Limit of Concrete Filled Steel Square Tubular Columns (in Japanese), *Journal Structural and Construction Engineering*, AIJ, No. 504, 103-110, Japan, February, 1998.

MLIT, *The 2015 Commentary on Structure Related Technical Standards for Buildings (in Japanese)*, Building Guidance Division, Housing Bureau, the Ministry of Land, Infrastructure and Transport (supervisor), June, 2015.

Mori, O., Noguchi, T., Fujimoto, T., and Morino, S., *US-Japan Cooperative Structural Research Project on Composite and Hybrid Structures (CFT-33) Hysteresis Characteristics Model of Concrete Filled Steel Tubular Columns (in Japanese)*, AIJ, Japan, September, 1998.